Source localization in shallow water using multi-frequency processing of shot data

Georgios Haralabus and Peter Gerstoft

The content of this document pertains to work performed under Project 41-2 of the SACLANTCEN Programme of Work. The document has been approved for release by The Director, SACLANTCEN.

Director

Source localization in shallow water using multi-frequency processing of shot data

Georgios Haralabus and Peter Gerstoft

Executive Summary: Single-frequency techniques which proved to be successful for source localization in deep-water are shown to be inadequate in littoral areas. To overcome this problem, the processing schemes need to be redesigned to extract and incorporate more information from the received signal and improve the estimates of parameters which describe the propagation channel. This report describes the use of multi-frequency processing methods in a global search scheme in which the source coordinates are estimated jointly with environmental parameters. The analysis is based on comparisons between modelled data and real data from explosive sources collected during a SACLANTCEN sea trial in the Mediterranean Sea, in October 1993.

The variability of geometric (source coordinates, array tilt), and environmental (water depth at the source and the receiver), parameters as a function of the number of frequencies is examined. It is shown that, for the particular data set, stable and reliable results are obtained when at least ten frequencies with the highest energy content are used. Beyond this "saturation" point the estimates remain relatively constant. Based on these observations, the localization performance of a multi-frequency version of the Bartlett processor is examined. It is demonstrated that insufficient knowledge of the propagation channel limits the resolution of the source location for both single-frequency and multi-frequency cases. The use of global inversion methods based on genetic algorithms for the joint optimization of environmental and geometric parameters is shown to considerably improve the localization performance of the processor.

The suggested multi-frequency methodology is related primarily to the way the received signal is processed and is independent of the geometry of the problem, therefore it can be equally well applied to both active and passive sonar.

Source localization in shallow water using multi-frequency processing of shot data

Georgios Haralabus and Peter Gerstoft

Abstract:

Multi-frequency processing methods are applied to real data generated by explosives to examine the variability of geometric and environmental parameter estimates. The frequencies are combined in an incoherent fashion and genetic algorithms are employed in an efficient global search scheme.

The source coordinates, the water depth at the source and the receiver location, and the tilt of the vertical array are estimated as functions of the number of frequencies processed. Using three different processing schemes, it is found that when less than ten frequencies are employed the estimates are unstable, whereas after this critical number a constant estimation level is attained.

The localization performance of a multi-frequency version of the Bartlett processor is also examined. The degradation of the results due to a non-optimized environment is demonstrated. The source resolution is shown to be improved when the search for the source coordinates incorporates simultaneous estimation of the environmental parameters.

Keywords: Multi-frequency processing, global search, localization

Contents

1

Introduction

Acoustic field inversion using matched field processing has been successfully used to determine both geoacoustic and environmental parameters. It has been found that the localization performance increases when selected waveguide parameters are determined simultaneously [1]. It has been shown that the stability of the parameter estimates is significantly improved when using data at a few well defined frequencies [2], [3]. A disadvantage of this approach is that the computational time increases linearly with the number of frequencies used in the inversion procedure. This study examines multi-frequency processing strategies for a transient signal in a mildly range-dependent, shallow water environment.

The data for this study were collected during a SACLANTCEN sea trial in 1993 [1]. More information about the experiment is given in the next section. Replica fields are calculated using the SNAP [4] adiabatic normal mode program. The environment can be described as a half-space divided into a water column, a sediment layer, and a semi-infinite sub-bottom (Fig. 1). It can be seen that this is a range dependent scenario in which the bathymetric difference between the source and the receiver is approximately 7 m. Comparisons between real and synthetic data are based on the Matched Field Processing (MFP) technique [5], [6]. This method compares the relative phase and amplitude of recorded signals with model predictions. To find the best fit between real and synthetic data, modelling and matching tools are incorporated into the SAGA [7] global inversion algorithm; a time-efficient, multi-dimensional search method based on genetic algorithms. In general, the following procedure is followed: a) The bounds of the parameters to be estimated are set based on *a priori* knowledge. Then, the environment is discretized and fed into SNAP. b) SNAP calculates the acoustic field at the receiver location. c) Real and simulation data (transformed in the frequency domain) are compared by means of an objective function. d) The above steps are repeated for the next chosen parameter set. The iteration procedure is controlled by SAGA. e) Statistical analysis and *a posteriori* probability plots of the obtained estimates are provided.

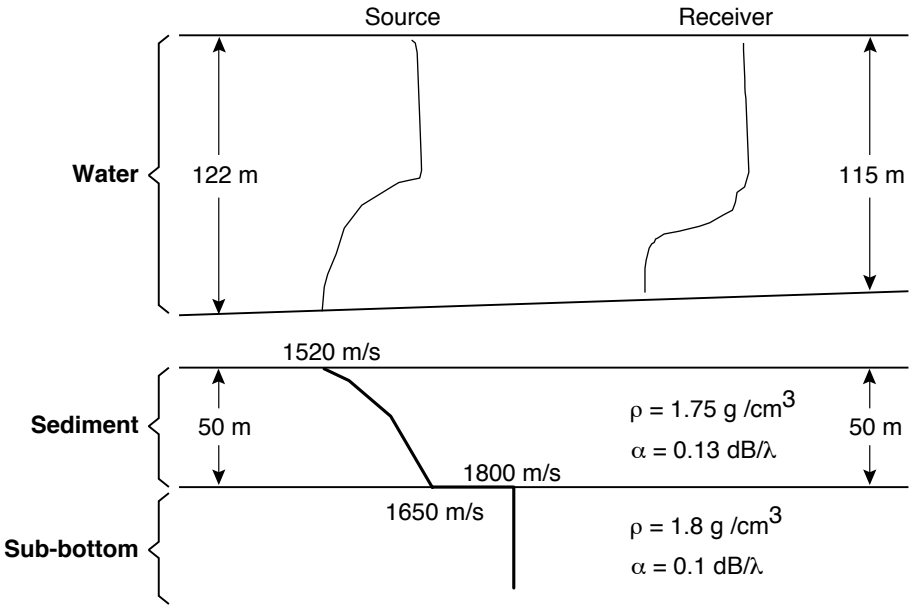

Figure 1: Measured sound-speed profile, bathymetry, and geoacoustic parameters for the experimental site north of the island of Elba.

2
Data collection

The data were collected during a SACLANTCEN sea trial north of the island of Elba in the Mediterranean Sea, in October 1993. Twenty-five explosive sound sources (SUS MK-61) were deployed during a triangular course with sides of 23 km. The propagated signals were received by a vertical array which was situated at the eastern apex of the triangle. Shot 5 was singled out for examination because this particular explosion rendered a better recording than the others, and is also investigated by Tolstoy et al [8], using different methods than those described in this paper. The number of hydrophones used and the sampling rate, were determined by the equipment on board the research vessel. For such practical reasons, in this experiment, the sampling frequency was 1000 Hz. Therefore, the maximum frequency is 500 Hz although it is known that the frequency band of explosions extends up to 10 kHz [9], [10]. Figure 2 shows the time series and the spectrum of the signal received on 32 hydrophones (with 2 m spacing) across the vertical array. The explosives were deployed from a ship which followed a preassigned path, so there is probably an offset between the registered coordinates and the site of the explosion. It would have been useful to have had additional sound velocity profile and bathymetric measurements along the propagation path because acoustic propagation is strongly dependent on these factors. Table 1 shows the five parameters considered in this study, the search interval for each, and the baseline values for this experiment.

Parameter	*S. range*	*S. depth*	*Depth at S.*	*Depth at R.*	*Tilt*
Interval	11–13 km	10–20 m	120–128 m	114–121 m	−3–3 m
Baseline	12.1 km	18 m	122 m	115 m	0 m

Table 1: Environmental, source and receiver parameters, and baseline model values. S and R denote source and receiver respectively.

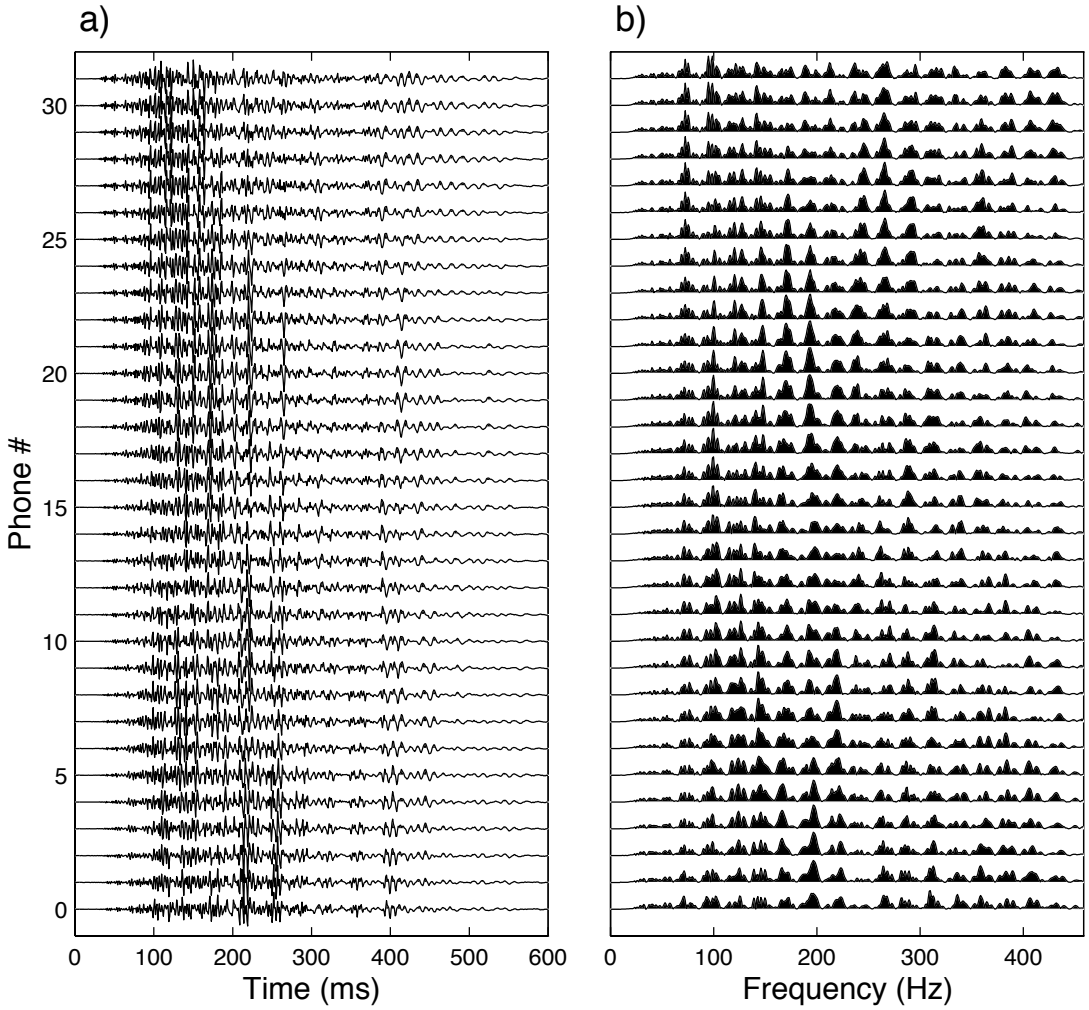

Figure 2: Time series (a) and frequency (b) spectrum of the signal received on the vertical array.

3
Objective function

Parameter estimation is treated as an optimization problem in which the algorithm searches for the model vector $\mathbf{m}$ which minimizes an objective function $\Phi(\mathbf{m})$. For a single frequency ω, let $\mathbf{d}(\omega)$ be the real data received on a vertical array of N hydrophones, and $\mathbf{p}(\omega)$ the data predicted from the simulation model. Real and synthetic data are related by the equation

$$\mathbf{d}(\omega) = \mathbf{p}(\omega) + \mathbf{n}(\omega) \tag{1}$$

where $\mathbf{n}(\omega)$ represents the noise. Since the synthetic data can be expressed as

$$\mathbf{p}(\omega) = \mathbf{w}(\omega, \mathbf{m}) s(\omega) \tag{2}$$

where $\mathbf{w}(\omega, \mathbf{m})$ is the transfer function of the acoustic medium and $s(\omega)$ is the deterministic source spectrum, Eq. (1) becomes

$$\mathbf{d}(\omega) = \mathbf{w}(\omega, \mathbf{m}) s(\omega) + \mathbf{n}(\omega) \tag{3}$$

or

$$\mathbf{n}(\omega) = \mathbf{d}(\omega) - \mathbf{w}(\omega, \mathbf{m}) s(\omega) \tag{4}$$

The $\mathbf{n}$ term includes primarily environmental noise and other factors of uncertainty, such as modelling and measurement inaccuracies. These factors of error are considered to be independent, random processes without burst-like quality. It is therefore reasonable to assume that $\mathbf{n}$ has a Gaussian distribution with zero mean and covariance matrix $\mathbf{C}$, i.e., $\mathbf{n} \in \mathrm{N}(0, \mathbf{C})$. Consequently, the real data $\mathbf{d}$ are also Gaussian

distributed, with mean $\mathbf{w}s$ and the same covariance matrix $\mathbf{C}$, i.e., $\mathbf{d} \in \mathrm{N}(\mathbf{w}s, \mathbf{C})$ (for simplicity the dependence on ω and $\mathbf{m}$ is omitted).

For complex data the probability density function is defined as:

$$p(\mathbf{d}) = \frac{1}{\pi^N |\mathbf{C}|} exp\left[-(\mathbf{d} - \mathbf{w}s)^\dagger \mathbf{C}^{-1}(\mathbf{d} - \mathbf{w}s)\right] \tag{5}$$

where N is the vector dimension, $\dagger$ is the complex-conjugate operator, and $|\mathbf{C}|$ denotes the deternimant of $\mathbf{C}$ matrix.

Assuming that the noise is spatially uncorrelated and an identical spectrum for each hydrophone, the cross-spectral covariance matrix can be written as $\mathbf{C} = \nu\mathbf{I}$, where the noise standard deviation ν depends only on frequency and $\mathbf{I}$ is the identity matrix.

In the case of broadband data, the processor incorporates individual frequencies in an incoherent fashion. Given the observed data sets $\mathbf{d}_l$ for different frequencies ω_l and assuming that they are uncorrelated with each other, the optimization problem is modified in order to find the model vector $\mathbf{m}$ which creates a replica field $\mathbf{w} = \mathbf{w}(\mathbf{m})$ which minimizes the logarithm of the likelihood function

$$M = \sum_{l=1}^{L} log(p(\mathbf{d}_l)) = \sum_{l=1}^{L} \left[-Nlog\pi\nu_l - \frac{1}{\nu_l}(\mathbf{d}_l - \mathbf{w}_l s_l)^\dagger(\mathbf{d}_l - \mathbf{w}_l s_l)\right] \tag{6}$$

where $l = 1, ..., L$ denotes the number of frequencies. When the expression for a harmonic point source $s_l = A_l e^{-i\theta_l}$ is substituted in Eq. (6) and one solves the equations $\frac{\partial M}{\partial A_l} = 0$ and $\frac{\partial M}{\partial \theta_l} = 0$, the estimate of the source signal becomes

$$\hat{s}_l = \frac{\mathbf{w}_l^\dagger \mathbf{d}_l}{\mathbf{w}_l^\dagger \mathbf{w}_l} \tag{7}$$

By substitution of Eq. (7) into Eq. (6), the likelihood function is modified as:

$$M = \sum_{l=1}^{L} \left[-N log \pi \nu_l - \frac{1}{\nu_l} \left(\mathbf{d}_l^\dagger \mathbf{d}_l - \frac{\mathbf{w}_l^\dagger \mathbf{d}_l \mathbf{d}_l^\dagger \mathbf{w}_l}{\mathbf{w}_l^\dagger \mathbf{w}_l} \right) \right] \tag{8}$$

For each frequency the cross-spectral covariance matrix of the actual data is calculated from the formula

$$\mathbf{R}_l = \mathbf{d}_l \mathbf{d}_l^\dagger \tag{9}$$

which implies that its trace is

$$\mathbf{tr}\mathbf{R}_l = \mathbf{d}_l^\dagger \mathbf{d}_l \tag{10}$$

Using Eq. (9) and (10), Eq. (8) becomes

$$M = \sum_{l=1}^{L} \left[-N log \pi \nu_l - \frac{1}{\nu_l} \left(\mathbf{tr}\mathbf{R}_l - \frac{\mathbf{w}_l^\dagger \mathbf{R}_l \mathbf{w}_l}{\mathbf{w}_l^\dagger \mathbf{w}_l} \right) \right] \tag{11}$$

This expression can be further simplified depending on the type of assumption which is made for the noise ν:

A) Assuming that ν is not constant, then by solving the equation $\frac{\partial M}{\partial \nu_l} = 0$, it is derived that

$$\hat{\nu}_l = \frac{1}{N} \left(\mathbf{tr}\mathbf{R}_l - \frac{\mathbf{w}_l^\dagger \mathbf{R}_l \mathbf{w}_l}{\mathbf{w}_l^\dagger \mathbf{w}_l} \right) \tag{12}$$

When Eq. (12) is substituted in Eq. (11) and unnecessary constants are removed, the exponential form of the likelihood operator is defined as the problem's objective function

$$\mathbf{\Phi} = \prod_{l=1}^{L} \left[\mathbf{tr}\mathbf{R}_l - \frac{\mathbf{w}_l^\dagger \mathbf{R}_l \mathbf{w}_l}{\mathbf{w}_l^\dagger \mathbf{w}_l} \right] \tag{13}$$

B) Alternatively, if ν is assumed constant, then directly from Eq. (11), the objective function becomes

$$\mathbf{\Phi} = \sum_{l=1}^{L} \left[\mathbf{tr}\mathbf{R}_l - \frac{\mathbf{w}_l^\dagger \mathbf{R}_l \mathbf{w}_l}{\mathbf{w}_l^\dagger \mathbf{w}_l} \right] \tag{14}$$

In both cases, the algorithm is searching for the model vector $\mathbf{m}$ which generates a synthetic field $\mathbf{w}(\mathbf{m})$ minimizing $\mathbf{\Phi}(\mathbf{m})$. In the present work we utilize Eq. (14). Notice that the second term in Eq. (13) and (14) is the expression for the Bartlett processor [5], i.e., for each frequency ω_l

$$\mathbf{B}_l = \mathbf{w}_l^\dagger \mathbf{R}_l \mathbf{w}_l = \left| \sum_{i=1}^{N} \mathbf{w}_{i,l}^\dagger \mathbf{d}_{i,l} \right|^2 \tag{15}$$

It should be noted that the same formulae apply when the real data used are created from the average of several time segments. Then, the covariance matrix can be calculated according to the formula

$$\hat{\mathbf{R}}_l = \frac{1}{K} \sum_{k=1}^{K} \mathbf{d}_l \mathbf{d}_l^\dagger \tag{16}$$

where K is the number of time segments.

Finally it should be mentioned that for each frequency, the objective function is based on the relative phase differences (weighted with pressure magnitude) across the elements of the receiving array. The L frequencies used in the inversion should be the ones that are best received on most hydrophones. To satisfy this condition, we calculate the array averaged spectrum in which each frequency bin corresponds to the summation of the energy components from all 32 hydrophones. Based on this calculation, the frequencies corresponding to the maximum values are selected.

4

Single-frequency parameter estimation

To demonstrate the need for multi-frequency analysis, one must provide evidence that single frequency algorithms are insufficient for accurate parameter estimates. As shown in this section, methods based on a single frequency lead to unstable results.

Here, two single-frequency scenarios for 146.5 and 194.3 Hz are examined. First the Fourier transform of the complete signal is calculated and then for each hydrophone the values corresponding to 146.5 and 194.3 Hz are selected. For each frequency, the covariance matrices are calculated according to Eq. (9). In both cases the search bounds and the baseline model are the same. The SAGA output is shown in Fig. 3. The vertical lines represent the baseline model and the *a posteriori* probability plots indicate the best parameter estimates.

It is obvious that the two predictions are quite different. Also, it is important to notice that the *a posteriori* probabilities have low standard deviation. This signifies that the algorithm *did* converge with the best solution for each frequency; in other words an increase in the number of iterations would not change the accuracy of these predictions. Key reasons for having inconsistent parameter predictions when different frequencies are processed are the insufficient knowledge of the propagation waveguide (e.g. sparsely collected environmental measurements), and the small number of time samples. The next step is to obtain more consistent estimates by combining information across the entire frequency spectrum.

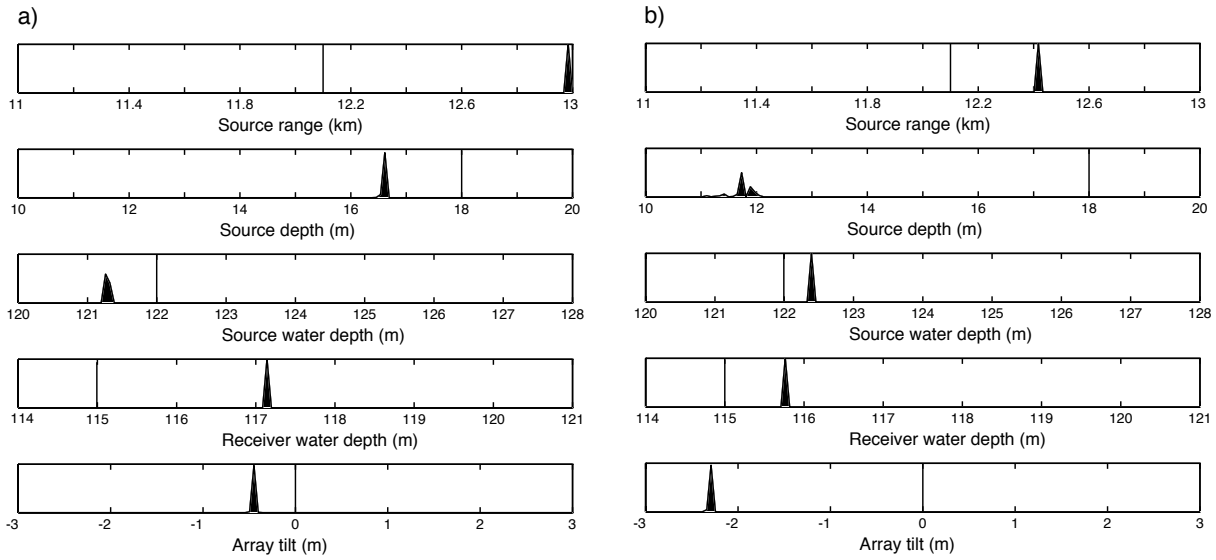

Figure 3: *A posteriori* distribution based on one frequency: a) 146.5 Hz, b) 194.3 Hz.

5

Multi-frequency parameter estimation

To overcome the inaccuracy of single-frequency estimates shown in the previous section, multi-frequency scenarios are investigated. The global inversion algorithm is now based on different data sets which include one to twenty five frequencies. These frequencies are selected according to energy content. Multi-frequency processing is performed in an incoherent fashion as indicated by Eq. (14). The object is to obtain estimates which are close to the baseline model and remain unchanged beyond a "saturation" point. These two conditions ensure reliable results and reduces computation time.

Initially, the calculation of cross-spectral covariance matrix is based on the Fourier transform of the complete set of time samples. For each frequency, the spectrum values are calculated for every hydrophone and from Eq. (9) the covariance matrix is estimated. This procedure is repeated for all frequencies and then the parameters are estimated using Eq. (14). The results from this process are shown in Fig. 4. The source coordinates correspond to the first two plots. Notice that when the number of frequencies is less than 10, the predictions for the source range and depth are unstable. Beyond this point the estimates reach a plateau which is close to baseline value. The predictions for the water depth at the source and the receiver do not follow the same trend. The first is overestimated for all frequency numbers while the second has sudden fluctuations around the critical point of 10 frequencies. Later it is shown that this fluctuation problem is eliminated by using different processing schemes. Finally, the array tilt demonstrates smooth convergence toward its mean position.

Obviously, the multi-frequency results are superior to the single-frequency ones because they are in general, stable and accurate. As expected, when the number of frequencies increases, the predictions gradually improve until they reach a stable value. This behaviour is intuitively more robust whether the estimates are close to the baseline model (cases of source coordinates and array tilt), or are not close to it (case of water depth at the source depth).

This analysis is based on the spectrum shown in Fig. 2. The stability of the estimates depends on the time variability of this energy distribution. To demonstrate this variability, the array averaged spectrogram [11] is calculated for a 256 ms time window which slides over the time domain with a 10 ms increment (Fig 5). It

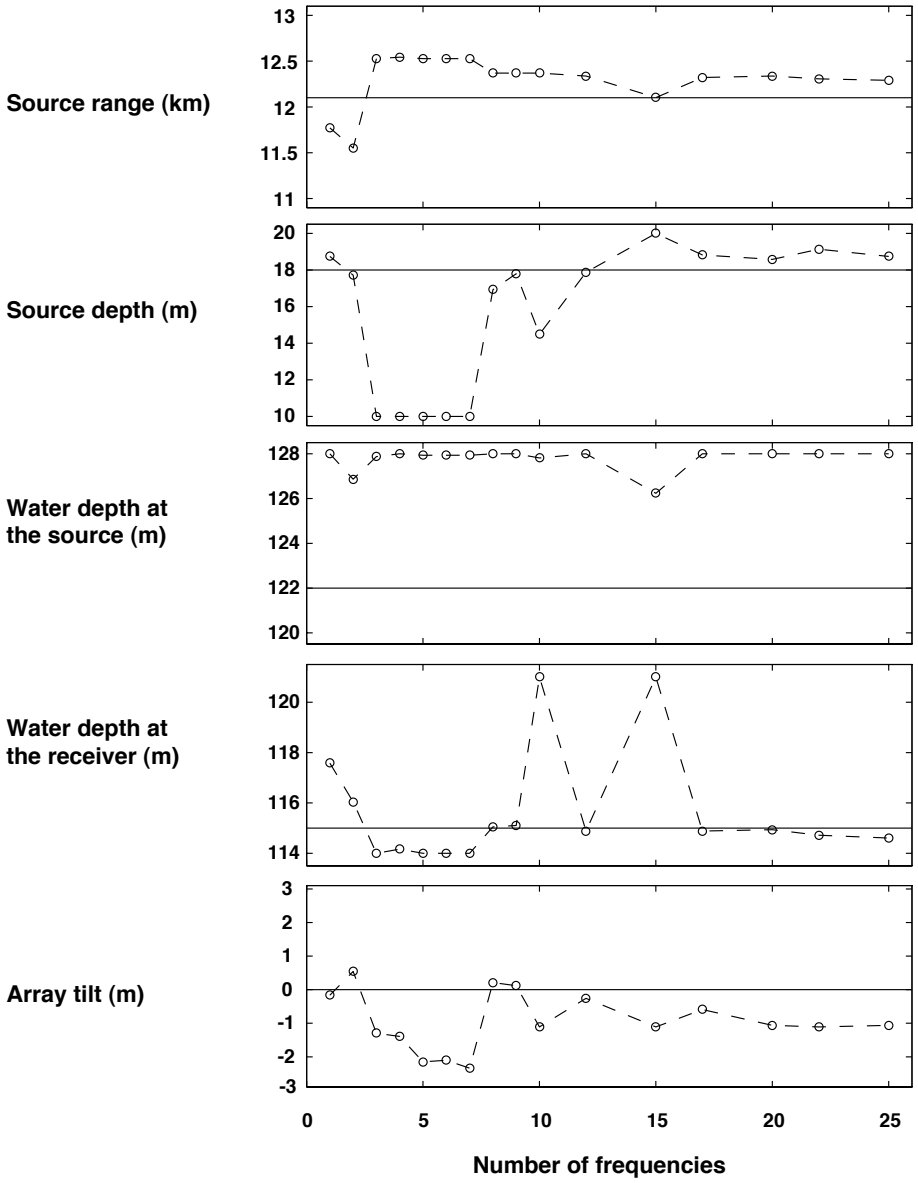

Figure 4: Parameter estimates as a function of the number of frequencies. Unmarked solid lines indicate the baseline model values. The whole time series is used and no averaging is performed.

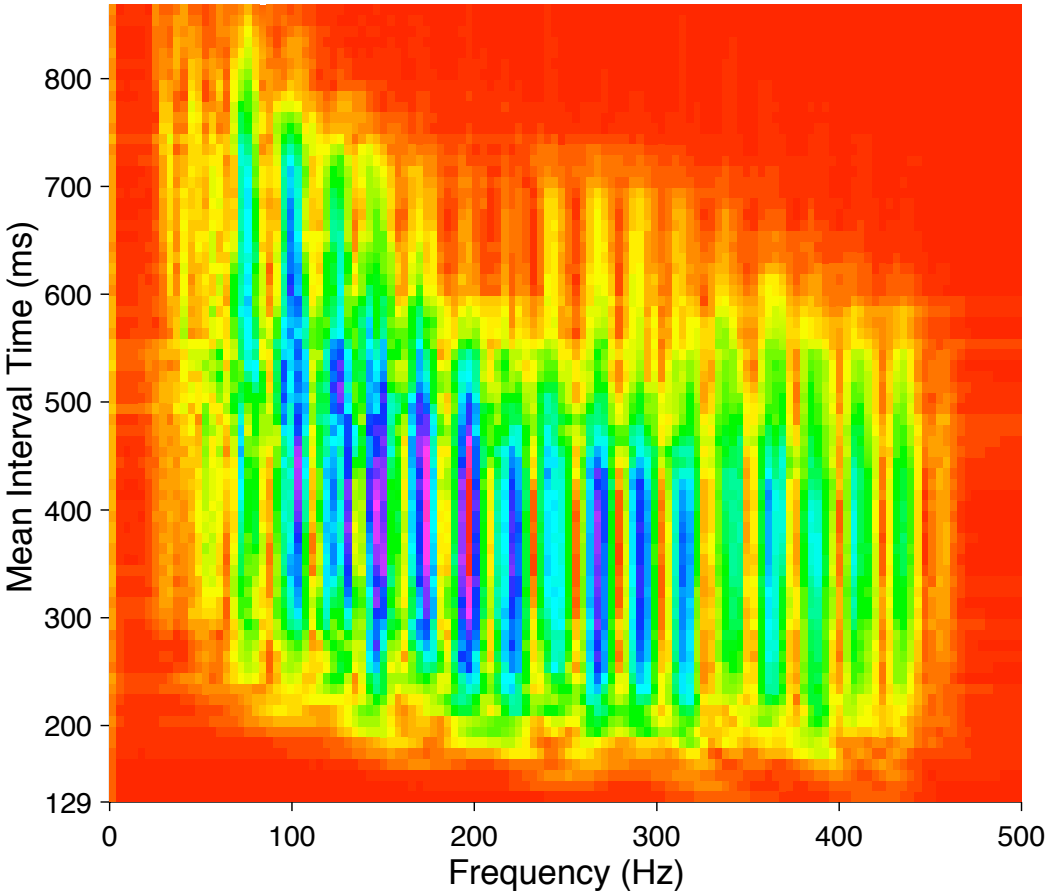

Figure 5: Array-averaged spectrogram.

can be seen that the energy content remains at the same level for only a short period (from 250 to 450 ms) corresponding to the high energy segment of the signal. Parameter estimates based on this time segment are expected to be very stable. To take advantage of this idea, two alternatives can be proposed: a) to process only the high energy segment of the returned signal between the 250th and the 450th time sample, and b) to use an averaging technique based on the entire time series. In both cases, the main idea is to eliminate or reduce the effect of the "noise-like" low-energy segment of the signal between the 450th and the 650th sample, and increase the influence of the strong signal.

In the first alternative, the estimates of the five parameters of interest are presented in Fig. 6. The source coordinates are shown in the first two plots. Similarly to the previous scenario, for less than 10 frequencies the estimates are unstable but beyond this critical point both parameters reach a plateau with small variations around the actual values. The most problematic parameter remains the water depth at the source location which is overestimated. The water depth at the receiver has a highly accurate estimate and the fluctuations observed in the previous method is eliminated. Finally, the array tilt slowly converges with its mean value zero. Comparing the two multi-frequency approaches, it is concluded that for this data set, exploiting only the high energy part of the shot is the preferred method as the results are more stable and the behavior of the processor is more predictable.

Proceeding with the second alternative, the information from both segments is combined using averaging techniques to balance the contribution of the low energy part of the signal. Here, the samples between 201 and 700 are selected. This series is divided into five non-overlapping segments using a 100-sample rectangular window. Covariance matrices are calculated for each segment and each frequency. The corresponding matrices are averaged to derive the final form of $\hat{\mathbf{R}}(\omega_l)$. The parameter estimation results are shown in Fig. 7. The critical number of frequencies remains at ten. It can be seen that the estimates for the source coordinates are very close to the expected values. The water depth at the source location is overestimated, as with the two previous cases. The estimate of the water depth at the receiver is exact and remains constant in the plateau zone. Finally, the array tilt, although it remains close to the nominal value, does not have as good an estimate as in the first method. In conclusion, the main characteristics of this approach are: a) transition regions which remain the same for all parameters, and b) plateau areas which are flatter than the ones in the previous cases. Both alternatives have comparable performance and are preferable to the original approach.

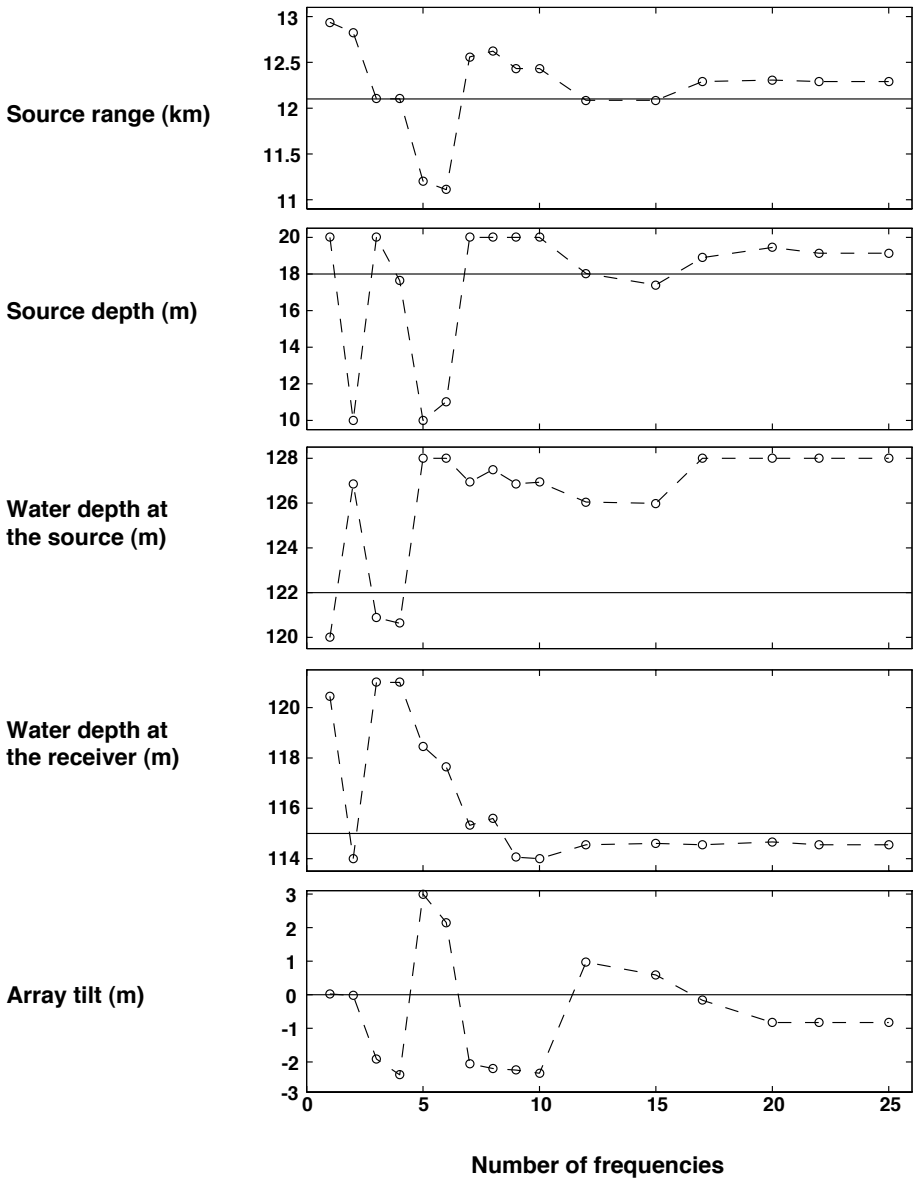

Figure 6: Parameter estimates as a function of the number of frequencies. Unmarked solid lines indicate the baseline model values. Only the high energy part of the signal is utilized (from the 250th to the 450th sample).

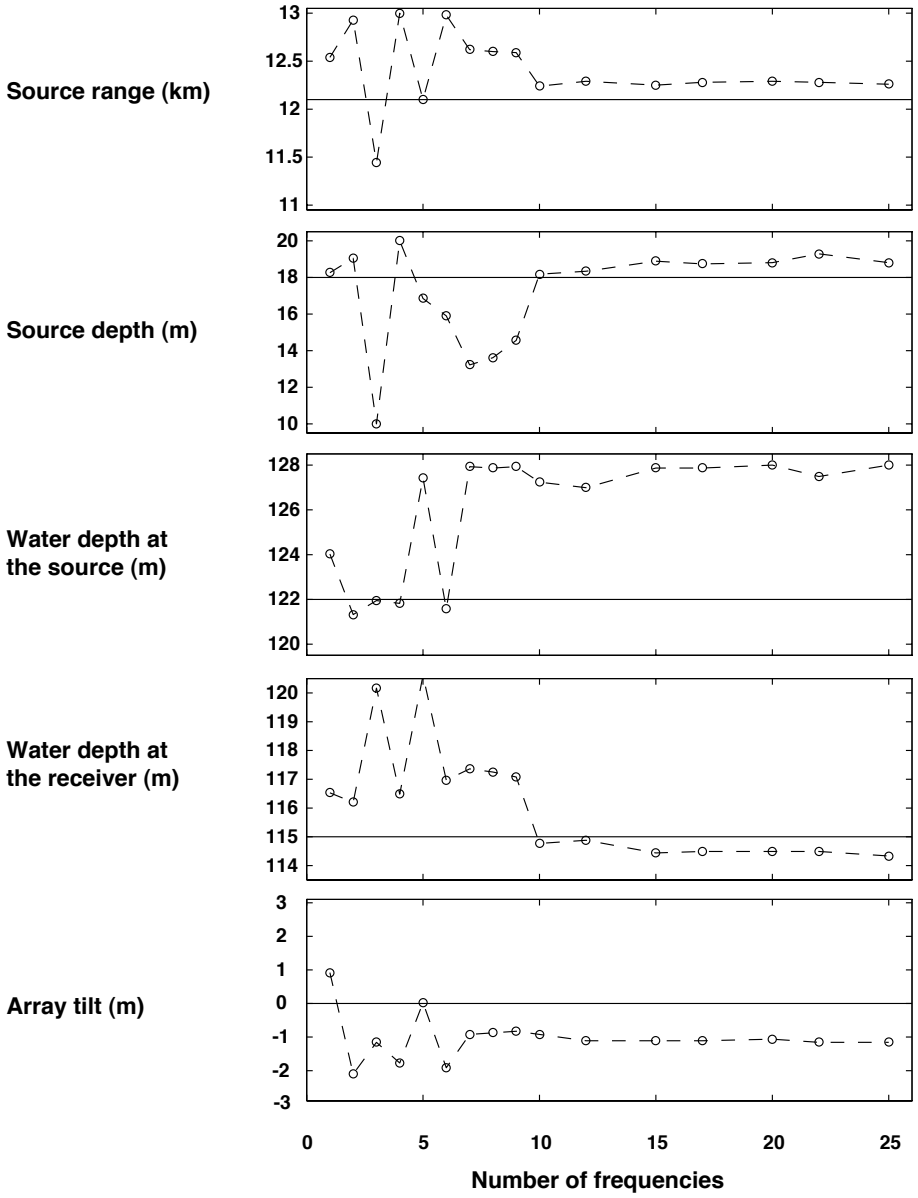

Figure 7: Parameter estimates as a function of the number of frequencies. Unmarked solid lines indicate the baseline model values. The time series is diveded into five segments and an averaging method is employed.

6

Multi-frequency matched field processing for source localization

Based on the same data set, this section focuses exclusively on the localization performance of the MFP technique for three reasons: a) in this experiment the source coordinates are known and thus the processor's performance can be easily verified, b) the prediction of the source location can be used as an indication of the accuracy with which the propagation channel is simulated, and c) to demonstrate the significance of the accurate knowledge of the environment in localization experiments.

The conclusions derived previously are employed to enhance the performance of the Bartlett-based processor. The goal is to find the most probable location for the underwater explosion based on comparisons between the signal received on the vertical array and synthetic data. Another way of demonstrating the outcome of this comparison is by plotting ambiguity surfaces which indicate the detection performance for all possible combinations of source range and depth. For the particular problem, the region of interest is from 11 to 13 km in range and from 10 to 20 m in depth. The estimated source coordinates are at a range of 12.1 km and depth 18 m.

The first ambiguity surface shown in Fig 8a represents the localization performance for the single-frequency case. The synthetic data are modelled according to the baseline model. The environmental parameters are assumed to be fixed, thus the inversion is confined to the source coordinates. The range is estimated at 12.1 to 12.3 km while the depth is underestimated at 11 to 16 m. This is not a satisfactory result since the area of uncertainty remains large. To improve this performance, additional frequencies are incorporated in the processor. The ten best frequencies are now selected because, as shown in section 5, this critical number yielded stable estimates for the particular data set. Again, the synthetic environment remains fixed and the comparison between real and synthetic data is based only on the source coordinates. Fig. 8b shows the ambiguity surface for this case. Although the estimated range is between 11.9 and 12.1 km, there is no depth resolution. The fact that the utilization of extra frequencies does not improve the processor's performance implies an inaccurately estimated synthetic field which causes the additional information due to combined frequencies to have a misleading effect on the processor. This is an indication that the parameters of the baseline model are not sufficiently accurate. So, the next step is to generate a more precise representation of the environment and then apply the same multi-frequency processor.

For this reason, the SAGA algorithm is employed as a pre-processor that estimates only the environmental parameters. The set which provides the best environmental fit takes the place of the baseline model and the ambiguity surface is recalculated. Now the outcome is considerably improved compared to both previous cases. As shown in Fig. 9a the most probable area for the source is around 12.25 km in range and between 16 and 19 m in depth.

To further improve the processor's performance, we modified the sequential optimization procedure to a global and simultaneous one. In other words, instead of first calculating the best possible environment and then searching for the most probable source location, now the inversion is jointly performed for all environmental and geometric parameters in a multi-frequency mode. The outcome is a five-dimensional a posteriori probability function. Figure 9b shows the distributions for the source coordinates. The only peak is around 12.25 km in range and 18 m in depth. As anticipated, the source localization performance is improved by using multi-frequency global inversion algorithms.

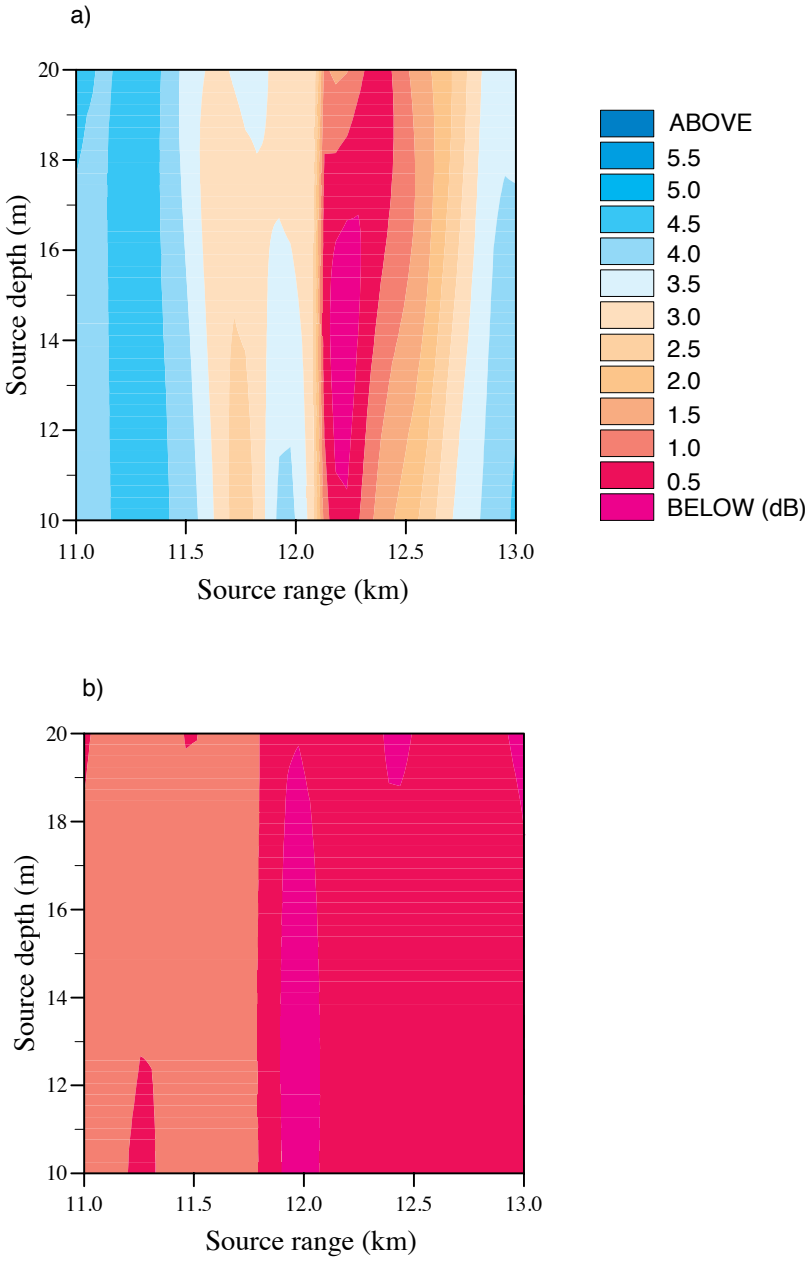

Figure 8: Ambiguity surfaces for localization performance based on the baseline model (non-optimized environment): a) single-frequency case, b) multi-frequency case. The source is located approximately at range 12.1 km and depth 18 m.

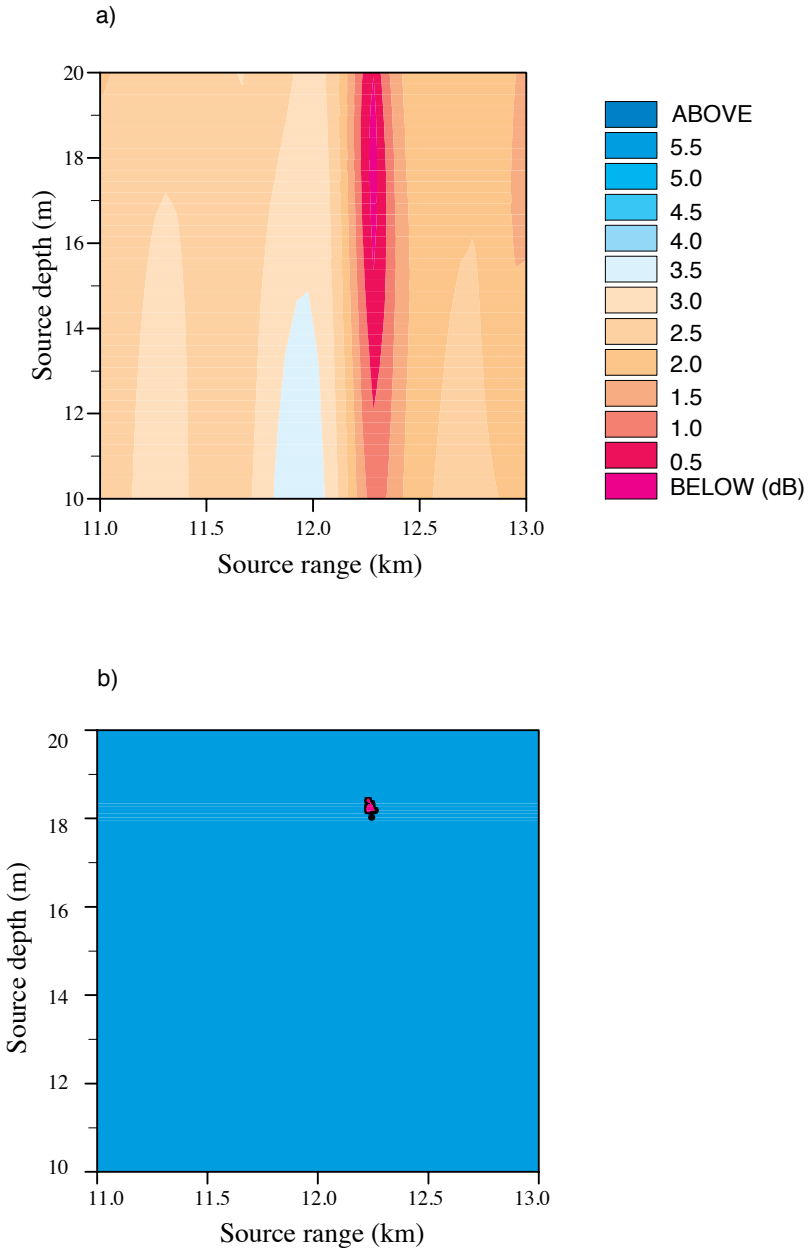

Figure 9: Multi-frequency localization performance: a) ambiguity surface based on the optimized environment, b) source coordinate distribution surface after global inversion. The source is located approximately at range 12.1 km and depth 18 m.

7

An alternative form of the objective function

As it is derived in section 3, the objective function is the summation of a number of frequency-dependent terms. Every term expresses the difference between the maximum power (perfect match) and the Bartlett power (actual match). Therefore, the value of the function Eq. (14) varies from zero to the sum of maximum power. This sum is an unnormalized quantity and the highest value it can assume depends not only on the number of frequencies involved but also on the energy content of each frequency. As the energy content of frequencies varies from case to case, direct comparison between different scenarios is difficult because every problem has its own bounds.

To overcome this inconsistency, a normalized version of the objective function was previously employed [12]. As seen in Eq. (17),

$$\mathbf{\Phi} = \sum_{l=1}^{L} \left[1 - \frac{\mathbf{w}_l^{\dagger} \mathbf{R}_l \mathbf{w}_l}{\mathbf{tr} \mathbf{R}_l \mathbf{w}_l^{\dagger} \mathbf{w}_l} \right] \tag{17}$$

each term is normalized with the trace of the covariance matrix, a quantity that represents the maximum power output for each frequency. Now the bounds of the objective function change from zero (perfect match) to the number of frequencies used (no match at all). Therefore, different scenarios which incorporate the same number of frequencies can be compared quantitatively as they have the same performance limits.

This normalization scheme has a major disadvantage: it eliminates the absolute difference between individual frequency components. Since every Bartlett term is normalized with its own maximum power, frequency components which encompass small amounts of energy are represented as equal to those belonging to the high energy part of the spectrum. Consequently, the parameter estimates can be very unstable, as demonstrated in Fig. 10. Here, the source coordinates are estimated using both the normalized Eq. (14) and the unnormalized Eq. (17) version of the objective function. The normalized-version results have unpredictable behaviour, especially, in the case of source depth where the estimate does not converge at all.

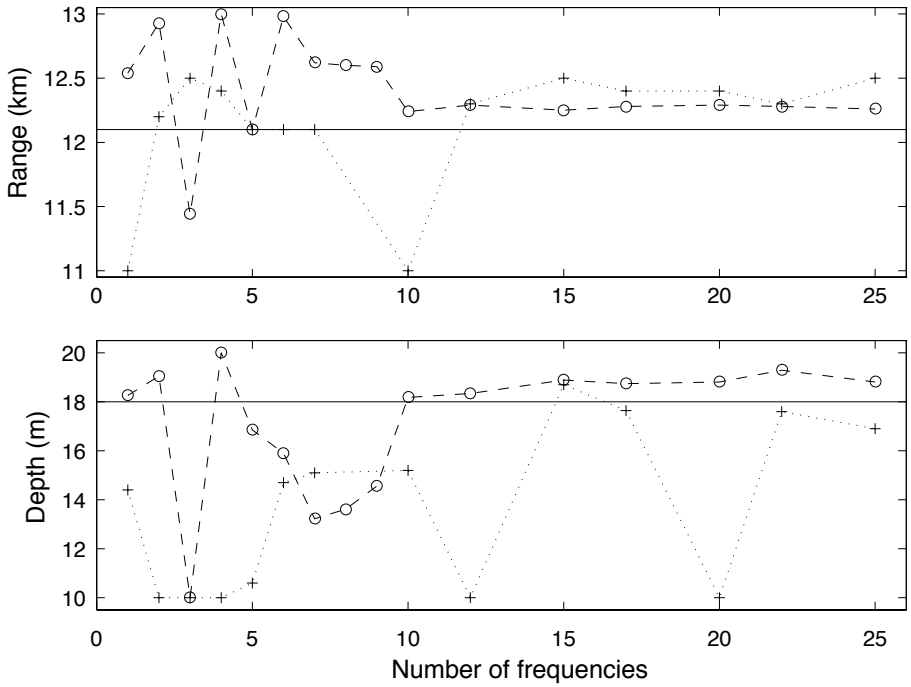

Figure 10: Parameter estimates for source range (a) and for source depth (b). Solid lines indicate the baseline model values. Lines designated with crosses represent the estimates of the normalized objective function. Lines designated with circles indicate the estimates of the unnormalized objective function.

The normalized version is suitable only when all the frequency components convey similar amounts of energy, and thus normalization is just a scaling process which does not affect the performance of the processor. When this condition is not fulfilled, or there is no sufficient *a priori* knowledge about the frequency components to be processed, the use of the unnormalized objective function is recommended.

8
Conclusions

In processing shot data in shallow water, it was found that single frequency parameter estimates are unstable and unreliable. The problem is overcome by using multi-frequency processing schemes. The frequency selection is based on high energy areas of the spectrum. On the basis of a limited data set, it is shown that as the number of frequencies is increased, the estimates remain unchanged beyond a critical point. This observation can be used to reduce computation time because it places an upper limit on the number of frequencies to be incorporated into the processor. The "saturation" point of ten frequencies found here is expected to vary for different data sets.

It is demonstrated that the localization performance of the MFP techniques is enhanced by using multi-frequency methods. Unless environmental modelling is accurate, the utilization of many frequencies does not necessarily imply improved source resolution. The combination of optimized environmental parameters and multi-frequency processing techniques enhances the performance of Bartlett-based processors.

It is found that when the inversion for the source coordinates is incorporated in a global search scheme which also allows geoacoustic parameters to be jointly optimized, the localization performance improves considerably. As this type of search is extremely time consuming, the application of an efficient global inversion method, such as genetic algorithms, is important.

References

[1] Gingras, D.F. and Gerstoft, P. Inversion for geometric and geoacoustic parameters in shallow water: Experimental results. *Journal of the Acoustical Society of America*, **97**, 3589–3598 (1995).

[2] Gerstoft, P. and Gingras, D.F. Parameter estimation using multi-frequency range-dependent acoustic data in shallow water. *Journal of the Acoustical Society of America*, **99**, 2839–2850 (1996).

[3] Hermand, J-P. and Gerstoft, P. Broadband multitone inversion of the Yellow shark data. *IEEE Oceanic Eng. (special issue on inversion techniques and the variability of sound propagation in shallow water), fall 96 (expected)* 1996.

[4] Jensen, F.B. and Ferla, M.C. *SNAP: The SACLANTCEN Normal-mode acoustic propagation model*, SACLANTCEN, SM–121. La Spezia, Italy, NATO SACLANT Undersea Research Centre, 1979.

[5] Tolstoy, A. *Matched Field Processing for Underwater Acoustics*. Singapore, World Scientific, 1993.

[6] Tolstoy, A. Review of matched field processing for environmental inverse problems. *International Journal of Modern Physics*, **3**, No. 4, 1992: 691–708

[7] Gerstoft, P. Inversion of seismo-acoustic data using genetic algorithms and *a posteriori* probability distributions. *Journal of the Acoustical Society of America*, **95**, 1994: 770–782

[8] Tolstoy, A. and Badiey, M. Shallow water bottom properties *via* matched field processing. *Oceans '95*, 1995: 1065-1070

[9] Urick, R.J. *Principles of Underwater Sound for Engineers*. New York, NY, McGraw-Hill, 1967.

[10] Weston, D.E. Underwater explosions as acoustic sources. *Proceedings of the Physical Society*, **76**, 1960: 233–249

[11] Oppenheim, A. V. and Schafer, R. W. *Discrete-Time Signal Processing*. Englewood Cliffs, NJ, Prentice Hall, 1989.

[12] Haralabus, G. and Gerstoft, P. Variability of multi-frequency parameter estimates in shallow water. *Proceedings of the 3rd European Conference on Underwater Acoustics*, FORTH, Crete, Greece, 1996.